

Protein hot spots at bio-nano interfaces

Nanotechnology has influenced the direction of research across the sciences, medicine, and engineering. Carbon nanotubes (CNTs) and, more recently, protein nanotubes (PNTs) and protein-inorganic nanocomposites have received considerable attention due to their unique nanostructures that can be utilized as a scaffold to house proteins or create nanowires. A shift towards protein-inorganic interactions has numerous applications from biosensors to biofuel cells and bio-based nanodevices. We examine several systems where protein hot spots, the active domains on proteins and the interactive dynamics in them, play a critical role in the interactions at the interface of these unique systems.

Gerald F. Audette^{a,*}, Stephanie Lombardo^a, Jonathan Dudzik^a, Thomas M. Arruda^b, Michal Kolinski^c, Slawomir Filipek^d, Sanjeev Mukerjee^b, Arunachala Mada Kannan^e, Velmurugan Thavasif, Seeram Ramakrishna^f, Michael Ching^g, Ponisseril Somasundaran^g, Sowmya Viswanathan^{h,*}, Resat S. Kelesi, and Venkatesan Renugopalakrishnan^{b,j,*}

^a Department of Chemistry, York University, Toronto, ON, M3J1P3, Canada

^b Center for Renewable Energy Technologies, Department of Chemistry and Chemical Biology, Northeastern University, Boston, MA 02115, USA

^c International Institute of Molecular and Cell Biology, 02-109 Warsaw, Poland

^d Faculty of Chemistry, University of Warsaw, ul. Pasteura 1, 02-093 Warsaw, Poland

^e Electronic Systems Department, Arizona State University, Mesa, AZ 85212, USA

^f NUS Nanoscience and Nanotechnology Initiative, National University of Singapore, Singapore 117576, Singapore

^g Department of Earth & Environmental Engineering, Langmuir Center for Colloids and Interfaces, Columbia University, New York, NY 10027, USA

^h Newton-Wellesley Hospital/ Partners Healthcare System, Newton, MA 02462, USA

ⁱ Department of Physics & Astronomy, Hunter College, The City University of New York, New York, NY 10021, USA

^j Children's Hospital, Harvard Medical School, Boston, MA 02115, USA

* E-Mail: audette@yorku.ca (G. F. Audette); sviswanathan1@partners.org (S. Viswanathan); v.renugopalakrishnan@neu.edu (V. Renugopalakrishnan)

The optimal design of interfaces between proteins and proteins, metal oxides, carbon nanotubes (CNTs), and other polymers is crucial to the design and construction of benign bio-nanodevices. To this end proteins, based on their desired physical properties and catalytic functions, must be adapted and optimized through genetic engineering, and nanoparticles must be made biocompatible¹.

In order to adapt proteins and nanoparticles for use in nanodevices, they must be interfaced with their biotic or abiotic partners² with or without active feedback control (Fig. 1). Such active feedback control is essentially negative feedback³⁻⁵ and is desirable at the nano-interface

as protein interactions are more unstable compared to other materials' interfaces. Extending active feedback control, in combination with biochemical data including hydrophobic surface area, electrostatic complementarity, etc., should facilitate better development of the bio-nano interface and reduce processing time with more accurate device manufacturing, testing, and calibration. From an economic standpoint, such devices will be considerably less costly, whether they are solar/bio-solar cells², sensors/bio-sensors, biofuel cells (BFCs), protein nanotubes^{6,7}, or nanoscale protein coated digital data storage media^{1,8-10}.

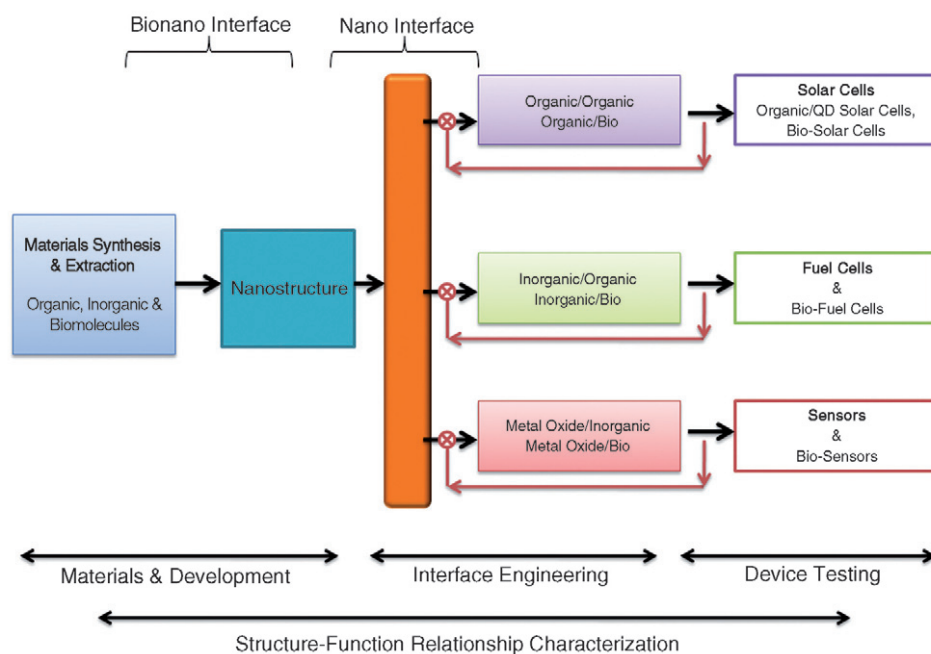


Fig. 1 A general overview of the integration flow for proteins into useable nanostructures and devices. Central to the development of optimized bionano interfaces is the detailed characterization of protein hot spots that establish the interaction between the protein and its nanostructured partner. Protein engineering is analogous to general materials development schemes, and is utilized to enhance the affinity, specificity, and robustness of the bionano interface. Optimized bionanocomposites are included in the final device to harness the desirable characteristics of both protein and nanostructured partners. Inclusion of active feedback (shown in red) mechanisms facilitates a more robust development of the bionano interface, which is centrally dependent on interfacial structure-function relationships.

While a significant amount of research has been directed towards understanding the interface in terms of the nanoparticles¹¹, the protein interface is mediated by molecular mechanisms, including dynamics that have not been fully unraveled. The study of these mechanisms often focuses on a selected subset of all interface residues, or “hot spots”, rather than the protein as a whole. These hot spots are crucial for recognition and binding, and are defined as residues that retard protein interactions if mutated. While no *in silico* mutagenesis efforts unambiguously identify hot spots, a number of predictive methods have been reported that identify residues that are likely to be a part of such interfaces¹²⁻¹⁵. Identified residues must then be systematically evaluated for synergetic or antagonistic effects to interfacial interactions. The challenge lies in capturing the engineered protein on active surfaces for the optimal expression of their function, thereby transforming them into functional and practical devices. It is also challenging to study events even on the scale of supramolecular clusters since most spectroscopic techniques tend to average the behavior of a group as a whole. The performance of an individual protein can be modified dramatically by the presence of others, due to a quorum effect.

Techniques are being developed to image single molecules and domains, as well as picosecond events. For example, AFM has been successfully used to generate clear images of pentacene and measure individual charges¹⁶. Even though chemical reactions at the single molecule level have been studied using scanning probe microscopy by Ertl¹⁷ and Somorjai¹⁸, as well as by using second harmonic generation

techniques and multi-step reactions by STM¹⁹, studies at the protein-water interface are yet to be probed by these techniques. On a supramolecular level, dynamics of the bacteriorhodopsin photocycle have recently been monitored in solution using picosecond time-resolved ultraviolet resonance Raman (UVRR) spectroscopy²¹. The 30 ps photodynamic process was detected with structural changes of at least two tryptophan and two tyrosine residues being monitored simultaneously. In addition, domain mobilities critical to enzymatic activity have been studied by Shapiro and colleagues using NMR/SRLS; average correlation times for domain motion were reported to be 10.4 ns versus 20.6 ns for global motions²². As protein domains often have different rates of motion, synchronization between different domains can conceivably be key for efficient processes at bio-inorganic interfaces.

Here we provide a perspective on several areas of emerging interest in which a protein interfaces with CNTs (glucose oxidase and laccase), and metal surfaces (pilin-derived protein nanotubes). We discuss the importance of these interfaces and highlight the role played by protein hot spots in the dynamics of protein-interface interactions and the development of these nanocomposites for bio-nano devices.

Protein-CNT interfaces: glucose oxidase and laccase

Glucose oxidase-based biosensors and BFCs

Glucose Oxidase (GOx) is a 160 kDa FAD containing homodimeric oxidoreductase (Fig. 2a)²² that catalyzes the oxidation of β -D-glucose

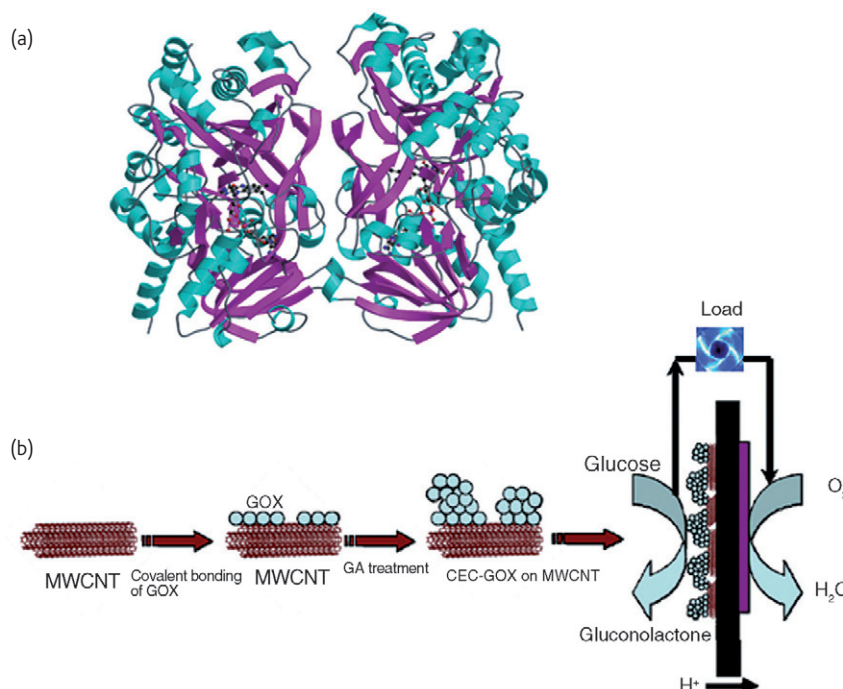


Fig. 2 Glucose oxidase and the generation of CECs (a) The GOx dimer of *A. niger* GOx, including the cofactor FAD²². The enzyme releases two electrons during the breakdown of β -D-glucose to gluconolactone; it is these electrons that are harnessed in GOx-based biosensors and BFCs. (b) A schematic representation of CEC-CNT nanocomposite generation utilizing GOx as the protein catalyst for the BFC anode. Reprinted with permission from⁷⁹. The GOx CECs better facilitate DET from the catalytic site of the enzyme to the CNTs for power generation; the GOx residues that interact with CNTs during CEC generation are a hot spot for interfacial interactions.

forming D-gluconolactone and hydrogen peroxide²³. GOx has been used in several diverse fields^{24–27}; since the mid-1960s, the medical industry's use of GOx has increased dramatically with the advent of biosensor technologies; primarily quantitative detection of blood glucose levels in diabetic patients^{28,29}. Early glucose biosensors included mediators to facilitate electron transfer from the redox centre of GOx to the electrode. This mediated electron transfer (MET) is enzyme-specific; however, redox species present in the electrolyte solution can interfere with the transfer of electrons²³. Current biosensors employ direct electron transfer (DET), based on the theory that the most efficient method to transfer electrons from GOx to an electrode is through direct attachment, thereby negating the mediator altogether. One such relay uses a poly-pyridine osmium-complex polymer to establish a path for the electrons to migrate from the FAD reaction centre to the electrode³⁰. The prevailing trend in biosensor development has been to narrow the gap between the enzymatic reaction center and the electrode to improve electron transfer efficiency.

The next generation of biosensors involves immobilizing GOx onto the electrode through surface functionalization. This relatively new paradigm has brought numerous inorganic materials to the forefront in determining which of their intrinsic properties can be best harnessed to yield the most efficient electrode for DET. Electrodes receiving the most attention include carbon nanotubes³¹, nanofibers³², and a range of nanoparticles (NPs)^{33–38}. Miniaturization of GOx biosensors in the form of implantable micro-devices for diabetic patients providing

continuous or periodic monitoring require that the device be self-powered, robust, biocompatible, and sensitive.

Biomolecular immobilization at surfaces can be achieved through either chemical (covalent) or physical (non-covalent) means³¹. Chemical immobilization is more likely to promote DET, while physical methods usually involve some form of MET via polymer matrices³⁵ or tethers³⁹. In most cases, functionalities must be introduced to the inorganic surface in order to provide a site to interact with its biomolecular counterpart. Various methods have been employed in functionalizing CNTs, CNFs, and NPs; one of which employs concentrated acids to form active carboxylic groups⁴⁰. The predominant method for GOx immobilization is through an amide bond formation involving the COOH functionalized inorganic surface and one of the 15 lysine or 22 arginine residues²². Another variation includes the covalent attachment of an FAD cofactor in order to reconstitute the dimer, for example using a FAD functionalized Au NP to immobilize GOx and enhance DET⁴¹. Interestingly, GOx reconstituted onto FAD-functionalized SWCNTs has been shown to transfer electrons more efficiently in comparison to covalent attachment of the holoenzyme⁴². A more recent trend has seen the development of immobilizing GOx in the form of crosslinked enzyme clusters (CECs)⁴³. This builds upon the high load capacity of nanostructures such as CNTs, due to their large surface area with the attachment of GOx CECs. The aim is to pack as much GOx on the inorganic scaffold as possible (Fig. 2), which should produce more power when implemented into a biosensor or BFC.

One area of concern with CNT-CECs is the lack of contribution of GOx molecules located at the core of the CEC. Moreover, challenges regarding GOx immobilization need to be addressed before BFCs are given serious consideration. Indeed, current strategies of GOx immobilization are generally non-specific, and targeted immobilization strategies will likely facilitate better enzyme clustering to address accessibility issues and promote DET. In addition, the thermal and structural stability of the enzyme is important as heat produced from the BFC could reach denaturing temperatures. The conductive nature of CNTs may facilitate heat transfer to the protein-inorganic interface, and incorporation of polyols has been shown to contribute to GOx's thermal stability in solution without interfering with function^{44,45}. In addition, glutaraldehyde, the crosslinker used in CEC generation is itself a possible protectant; Lopez-Gallego and colleagues⁴⁵ determined that the multiple site covalent attachment, provided by one molecule of glutaraldehyde and paramount to creating the EC, was 400 times more stable in comparison to an individual molecule of GOx. Stability is needed in order to expand the lifetime of the cell which at present remains 97 % active after a GOx-LHT-carbon-nanofiber biocomposite cell is continuously operated for 100 hours³². Clearly, despite these recent advances, significant work remains to develop GOx bio-nanocomposite interfaces for producing efficient and robust BFC and biosensors.

Laccase-based biocathodes

Laccase, a copper-containing oxidoreductase is redox active to a range of substrates including diphenols, aryl diamines, and aminophenols, but most importantly is selective toward the reduction of dioxygen to water via a four electron pathway⁴⁶. Its active site contains four spectroscopically distinct Cu ions, one type 1 (T1), one type 2 (T2), and two type 3 (T3), and based on redox potentials the most common laccase sources for BFCs are the *Rhus vernicifera* (E_0 394 - 434 mV, pH 7.0) and *Trametes versicolor* (E_0 780 - 800 mV, pH 4.0) enzymes. Noting that in BFCs it is imperative that the protein/electrode boundaries are well understood to ensure maximum cell efficiency, laccase is catalytically suited for biocathodes due to its high activity toward full 4-electron reduction, with successful applications of DET and MET reported in the literature.

For DET to occur in laccase-based biocathodes, the enzyme must be immobilized stably through a variety of methods onto the surface of the electrode and must be oriented such that the T1 Cu is within the electron tunnelling distance. For instance, Ivnitski and Atanassov⁴⁷ used a physical adsorption via a combination of glutaraldehyde and polyethylenimine to cross link laccase to carbon electrodes rich in hydrophilic groups. Not only were they able to detect bioelectrocatalytic reduction of dioxygen, but they also observed two separate redox peaks (at 99 and 530 mV) under anaerobic conditions, attributing them to the T2/T3 and T1 Cu centers, respectively. This observation is unique as they were not only able to determine a formal potential for the trinuclear Cu center potentiostatically, but they also observed electron tunnelling directly

to the trinuclear center, which is deeply embedded. Covalent coupling methods for laccase immobilization have recently been reported by using thiol rich compounds such as α -lipoic acid⁴⁸ and 4-aminothiophenol⁴⁹ on Au electrodes. In the former, laccase was chemically tethered to nanoporous Au electrodes by utilizing a Au-S bond at the Au interface, resulting in immobilized laccase which is in close enough proximity to allow for tunnelling. Interestingly, this covalent coupling method may have been slightly enhanced by the physical adsorption of laccase directly onto the nanoporous gold. *T. versicolor* laccase contains eight lysine residues, four of which are on or near the surface which can conceivably supply a bridge to the nanoporous Au via the N-terminus of the side chain. The Michaelis-Menten type kinetic analysis by Qiu and coworkers^{48,50} revealed that smaller (μm size) nanoporous Au particles improved catalytic efficiency, possibly by exposing the active site to the substrate and enhancing mass transfer.

Laccase cathodes employing DET are typically limited to a maximum of a monolayer of enzyme, which in turn limits the power output of the electrode. Increasing the surface area of the electrode using CNTs and NPs could potentially alleviate this limitation. Such has been demonstrated by a number of investigators^{51,52} with some success. However, power densities such as those obtained for a laccase cathode and carbon/ascorbate anode are routinely on the order of μWcm^{-2} ⁵². It may also be possible to utilize laccase CECs to increase power outputs; this possibility has not yet been investigated, although we are moving in that direction. Therefore, to realize the full potential of BFCs, investigators are also considering MET to increase the total enzyme content on the electrode and hence the power density. MET mediators, whether diffusional or wired, allow for the catalyst layer to be much thicker (100 μm) than monolayers obtained for DET⁵³, although the presence of an added electron transfer step in MET does introduce possible inefficiencies. Potential mediators are selected after considering a variety of properties, and are expected to be primarily oxidized or reduced at electrode potentials greater than or below the redox potential of the mediator, respectively. The resulting mixed potential then represents the open circuit potential of a cell employing two such mediated electrodes, and must be chosen with a redox potential close to the potential of the enzyme. Current state of the art mediators involve osmium-based organometallic moieties tethered to a polymer backbone such as polyvinyl imidazole⁵⁴, where the redox potential can be tuned by changing the substituents on the Os complex. Recently, Hudak *et al.*⁵⁵ demonstrated an H_2/O_2 fuel cell which operated with a maximum power density of 0.7 mWcm^{-2} using Os mediators on a laccase biocathode. Further, oxygen reduction current densities obtained were on the order of 1 - 10 mAcm^{-2} , several orders of magnitude higher than that obtained for DET biocathodes⁵⁴. Electrokinetic analysis of Os mediator/laccase biocathodes indicate biomolecular rate constants for mediation were between 250 - $9.4 \times 10^4 \text{ s}^{-1} \text{ M}^{-1}$ when the redox potentials of the mediator and laccase are in close proximity or respectively far apart⁵⁶. Such values were used to determine the

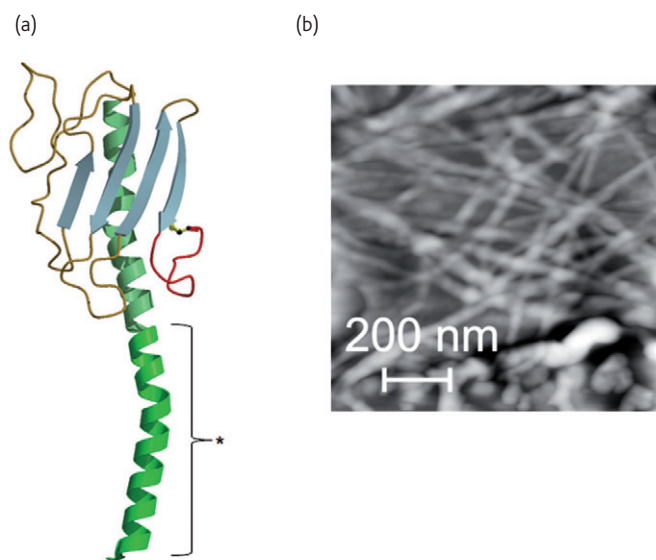


Fig. 3 The type IV pilin and pilin-derived PNTs. (a) The monomeric pilin from *P. aeruginosa* strain K75. Native T4P are generated from full-length pilins, in which the highly conserved and highly hydrophobic N-terminal region of the α -helix (shown in green). Truncation of the first 28 residues of this N-terminal helix (denoted with an asterisks) greatly enhances protein solubility⁷²⁻⁷⁴; it is from these truncated pilins that PNTs are oligomerized^{6,77}. The receptor binding domain (RBD), shown in red, has been identified as a hot spot for T4P/pilin/PNT interactions with biotic and abiotic surfaces. (b) An AFM image of pilin-derived PNTs oligomerized on a alkylthiol modified Au(111) surface. Reprinted with permission from⁷⁷. While PNT oligomerization is induced by the alkyl chain^{6,77}, the pilin RBD likely makes several critical stabilizing interactions with the modified Au(111) surface.

optimal mediator redox potential of 0.66 V vs NHE and a mediator structure was proposed to achieve this value⁵⁷.

Protein-metal interfaces: pilin-derived protein nanotubes

Another system bridging the protein-nano interface is the type IV pilus (T4P) of *Pseudomonas aeruginosa*. *P. aeruginosa*, a gram-negative opportunistic pathogen, mediates cell contact through T4P, 1000 – 4000 nm long fibrous structures that extend from the poles of the bacterium and attach to glycolipid receptors on the host cell⁵⁸⁻⁶³. T4P are robust structures, with extension/retraction rates of $\sim 0.5 \mu\text{m/s}$ ^{64,65} and resisting shear forces over 100 pN^{66,67}; T4P are also versatile structures, being involved in DNA uptake⁶⁸ and attachment to abiotic surfaces⁶⁹⁻⁷¹. T4P are polymers of a single monomeric subunit, the type IV pilin. Structural studies of several strains of bacterial pilins have revealed a common structural architecture (Fig. 3a)^{63,72-75}, with the C-terminal receptor binding domain (RBD) mediating interactions with cellular receptors⁵⁹⁻⁶¹ and abiotic surfaces⁶⁹⁻⁷¹. Interestingly, the RBD consists primarily of main-chain atoms⁷²⁻⁷⁶, thereby imposing conformational restraints to RBD interactions^{72,76}; clearly this region of the protein is a hot spot for interactions. Recently, a recombinantly expressed RBD was observed to bind stainless steel, with a ~ 2 -fold greater adhesive force for grain


boundaries⁷¹. While the exact interaction between the RBD and the steel surface is unclear, it likely results from stabilization or electron sharing from the metal surface in addition to the expected van der Waals interactions⁷¹. One possible way to increase adhesion robustness is to design substrates with appropriate grain boundaries, or even design a variety of substrates with designed ridges, valleys, edges, and nanohills/holes.

The first 28 N-terminal residues of the *P. aeruginosa* pilins are utilized as an oligomerization domain for the native T4P (Fig. 3a)^{7,62,63,72,75}, however truncation of these residues liberates a highly soluble monomeric pilin that retains the receptor-binding characteristics of the intact protein⁷²⁻⁷⁴. Interestingly, the truncated pilin monomers were found to aggregate in the presence of hydrophobic compounds into structures similar in morphology and diameter (~ 6 nm) to T4P, although much longer in overall length⁶. As these pilins do not inherently contain the exposed α -helix, upon oligomerization they form structures that can be described as protein nanotubes (PNTs). PNTs have been found to bind to stainless steel in a similar, though slightly weaker manner to the binding observed for T4P^{70,71}. Similar to T4P, the interaction between the PNT and steel is mediated by the tip-associated RBD. The attractive force between the RBD and steel is in the range of 26 – 55 pN/molecular interaction and the PNT-stainless steel adhesive force ranges from 78 – 165 pN/PNT-steel interfaces⁷¹.

The utilization of PNTs in nanoelectronics requires adherence of the PNTs to an abiotic surface. We recently reported the development of a novel biometallic interface in which pilin-derived PNTs could be grown from an alkylthiol-constrained Au surface (Fig. 3b)⁷⁷. Surface-constrained PNTs were several micrometers in length and appeared to cluster into filaments of ~ 6 PNTs when analyzed with AFM⁷⁷. It is likely that this interaction is stabilized, if not directly mediated, by the RBD of the terminal pilin monomer of the PNT with either the surface itself, or the thiol-constrained hydrophobe on the surface, and area of current investigation. These observations lead into the development of surface-constrained PNTs as promising bio-nanocomposites as the protein component of a biometallic interface can be modified through protein engineering to enhance the robustness of the system as well impart desired physicochemical properties to the system.

Concluding remarks

The development of optimized nanodevices for implantable systems, biosensors, etc., requires the integration of the unique strengths and capabilities of its biotic and abiotic partners. This integration is dependent upon an optimal interface between the protein and its partner protein or inorganic substrate. For proteins, such interfaces are achieved through hot spots of residues that provide selectivity and specificity to the interaction. Characterizing novel protein-inorganic interfaces provides the possibility of developing nanodevices that have improved electron transfer for

DET-based devices, or are tailored to attract targeted cells or molecules, giving rise to implantable devices such as glucose or cholesterol monitors. It is also possible that these tailored bio-nanocomposites could be used in the treatment of cancers, wherein such implantable devices could contain nanoparticles storing targeted therapeutics or radiation for the slow necrosis/lysis of the tumor cells. The detailed characterization and optimization of protein hot spots will lead to improved interfacial interactions, stable catalytic electron transfer, in turn leading to both a greater understanding of the molecular requirements of such interfaces and more readily integrated devices, BFCs, and biosensors. 

Acknowledgements

GFA gratefully acknowledges financial support from the Natural Sciences & Engineering Council of Canada (NSERC), the Canadian Foundation for Innovation and York University. VR wishes to thank Dr. Bernardo Barbiellini, Northeastern University, Boston, MA, USA for helpful discussions, and expresses his thanks to NSF, Wallace H Coulter Foundation, USAFOSR, ONR, NIH and Harvard Medical School. AMK would like to thank Arizona State University for financial support through ASU-ITESM (Mexico) Renewable Energy grant. SM would like to express his thanks to AFOSR funded MURI on Enzymatic Fuel Cells lead by UNM for financial support.

REFERENCES

1. Renugopalakrishnan, V., and Lewis, R. V., *Bio-nanotechnology: Proteins to Nanodevices*, Springer BV, Dordrecht, The Netherlands (2006).
2. Tatke, S. S., et al., *Nanotechnology* (2004) **15**, S684.
3. Keles, R., *Aircraft Design* (2000) **3**, 1.
4. Keles, R. *Active control of vortex shedding in the far wake of a cylinder*, 15th ASCE Engineering Conference, June 2-5, Columbia University, N.Y., pp.1-13 (2002).
5. Keles, R., and Chen, L., *Feedback control of vortex shedding in the wake of a circular cylinder: Active control of transition to turbulence in the wake of a cylinder*. The 48th Annual Meeting, APS-Fluid Dynamics, Nov. 19-21, Irvine, C.A., 2025-2026 (1995).
6. Audette, G. F., et al., *Nano Lett* (2004) **4**, 1897.
7. Audette, G. F., and Hazes, B., *J Nanosci Nanotech* (2007) **7**, 2222.
8. Renugopalakrishnan, V., et al., *Inter J Quantum Chem* (2003) **95**, 627.
9. Renugopalakrishnan, V., et al., *J Nanosci Nanotechnol* (2005) **5**, 1759.
10. Khizroev, S., et al., *Bulletin Mat Res Soc* (2008) **33**, 864.
11. Nel, A. E., et al., *Nature Mater* (2009) **8**, 543.
12. DeLano, W. L., *Curr Opin Struct Biol* (2002) **12**, 14.
13. Moreira, I. S., et al., *J Comp Chem* (2007) **28**(3), 644.
14. Darnell, S. J., et al., *Proteins* (2007) **68**, 813.
15. Cho, K. I., et al., *Nucleic Acids Res* (2009) **37**(8), 2672.
16. Gross, L., et al., *Science* (2009) **325**, 1110.
17. Ertl, G., *Angew Chem Int ed* (2008) **47**, 3524.
18. Somorjai, G., *Appl Surf Sci* (1997) **121**, 1.
19. Elmansa, J. A. A. W., *Mater Today* (2009) **12**(7-8), 34.
20. Mizuno, M., et al., *J Phys Chem B* (2009) **113**(35), 12121.
21. Shapiro, Y.S., et al., *J Phys Chem B* (2009) **113**(35), 12050.
22. Wohlfahrt, G., et al., *Acta Crystallog* (1999) **D55**, 969.
23. Wong, C. M., et al., *Appl Microbiol Biotechnol* (2008) **78**, 927.
24. Field, C. E., et al., *J Food Sci* (1986) **51**, 66.
25. Vemulapalli, V., et al., *Cereal Chem* (1998) **74**, 439.
26. Pickering, G. J., et al., *Food Res Int* (1998) **31**, 685.
27. Uppoor, R., et al., *Pharm Dev Technol* (2001) **6**, 31.
28. Newman, J. D., and Turner, A. P. F., *Biosensors Bioelectronics* (2005) **20**, 2435.
29. Clark, L. Jr., and Lyons, C., *Ann NY Acad Sci* (1962) **102**, 29.
30. Mano, N., et al., *J Amer Chem Soc* (2003) **125**, 6588.
31. Tsai, Y. C., et al., *Langmuir* (2005) **21**, 3653.
32. Vamvakaki, V., et al., *Anal Chem* (2006) **78**, 5538.
33. Thibault, S., et al., *Microchim Acta* (2008) **163**, 211.
34. Libertino, S., et al., *Sensors* (2008) **8**, 5637.
35. Cao, H., et al., *Electroanalysis* (2008) **20**, 2223.
36. Cao, Z., et al., *Anal Lett* (2007) **40**, 2116.
37. Yang, X., et al., *IEEE Sensors J* (2007) **7**, 1735.
38. Landoulsi, J., et al., *Electrochem Acta* (2008) **54**, 133.
39. Mao, F., Mano, N. & Heller, A. J. *Amer. Chem. Soc.* **125**, 4951-4957 (2003).
40. Saito, T., et al., *Physica B* (2002) **323**, 280.
41. Xiao, Y., et al., *Science* (2003) **299**, 1877.
42. Liu, J., et al., *Electroanalysis* (2005) **17**, 38.
43. Fischback, M. B., et al., *Electroanalysis* (2006) **18**, 2016.
44. Eremin, A. N., et al., *Appl Biochem Microbiol* (2001) **37**, 578.
45. Lopez-Gallego, F., et al., *J Biotechnol* (2005) **119**, 70.
46. Solomon, E. I., et al., *Chem Rev* (1996) **96**, 2563.
47. Ivnitski, D., and Atanassov, P., *Electroanalysis* (2007) **19**, 2307.
48. Qiu, H., et al., *J Phys Chem C* (2008) **112**(38), 14781.
49. Shleev, S., et al., *Electroanalysis* (2006) **18**(19-20), 1901.
50. Qiu, H., et al., *J Phys Chem C* (2009) **113**(6), 2521.
51. Rahman, M. A., et al., *Anal Chem* (2008) **80**(21), 8020.
52. Zheng, W., et al., *Chem Phys Lett* (2008) **457**(4-6), 381.
53. Barton, S. C., et al., *Chem Rev* (2004) **104**, 4867.
54. Barton, S. C. et al., *J Phys Chem B* (2001) **105**(47), 11917.
55. Hudak, N. S., et al., *J Electrochem Soc* (2009) **156**(1), B9.
56. Ivnitski, D., et al., *Small* (2008) **4**(3), 357.
57. Gallaway, J. W., and Calabrese Barton, S. A., *J Am Chem Soc* (2008) **130**(26), 8527.
58. Lyczak, J. B., et al., *Microbes Infect* (2000) **2**, 1051.
59. Govan, J. R. W., and Deretic, V., *Microbiol Rev* (1996) **60**, 539.
60. Lee, K. K., et al., *Mol Microbiol* (1994) **11**, 705.
61. Yu, L., et al., *Infect Immun* (1994) **62**, 5213.
62. Craig, L., et al., *Nat Rev Microbiol* (2004) **2**, 363.
63. Burrows, L. L., *Mol Microbiol* (2005) **57**, 878.
64. Mattick, J. S., *Annu Rev Microbiol* (2002) **56**, 289.
65. Skerker, J. M., and Berg, H. C., *Proc Natl Acad Sci USA* (2001) **98**, 6901.
66. Maier, B. et al., *Proc Natl Acad Sci USA* (2002) **99**, 16012.
67. Merz, A. J., et al., *Nature* (2000) **407**, 98.
68. Dubnau, D., *Annu Rev Microbiol* (1999) **53**, 217.
69. Miller, M. J., and Ahearn, D. G., *J Clin Microbiol* (1987) **25**, 1392.
70. Giltner, C., et al., *Mol Microbiol* (2006) **59**, 1083.
71. Yu, B., et al., *J Bio-nanoscience* (2007) **1**, 73.
72. Hansen, J. K., and Forest, K. T., *J Mol Microbiol Biotechnol* (2006) **11**, 192.
73. Hazes, B., et al., *J Mol Biol* (2000) **299**, 1005.
74. Audette, G. F., et al., *Biochemistry* (2004) **43**, 11427.
75. Craig, L., et al., *Mol Cell* (2003) **11**, 1139.
76. Kao, D. J. et al., *J Mol Biol* (2007) **374**, 426.
77. Lombardo, S., et al., *J Bio-nanosci* (2009) **3**, 65.
78. Reguera, G., et al., *Appl Environ Microbiol* (2006) **72**, 7345.
79. Kannan, A. M., et al., *J Nanosci Nanotechnol* (2009) **9**(3), 1665.